

Long-time and unitary properties of semiclassical initial value representations

C. Harabati¹, J. M. Rost¹, and F. Grossmann²

¹*Max-Planck-Institute for the Physics of Complex Systems,
Nöthnitzer Strasse 38, D-01187 Dresden, Germany*

²*Institute for Theoretical Physics, Dresden University
of Technology, D-01062 Dresden, Germany*

(Dated: November 9, 2018)

Abstract

We numerically compare the semiclassical “frozen Gaussian” Herman-Kluk propagator [Chem. Phys. **91**, 27 (1984)] and the “thawed Gaussian” propagator put forward recently by Baranger et al. [J. Phys. A **34**, 7227 (2001)] by studying the quantum dynamics in some nonlinear one-dimensional potentials. The reasons for the lack of long time accuracy and norm conservation in the latter method are uncovered. We amend the thawed Gaussian propagator with a global harmonic approximation for the stability of the trajectories and demonstrate that this revised propagator is a true alternative to the Herman-Kluk propagator with similar accuracy.

I. INTRODUCTION

The inclusion of quantum effects into classical dynamical calculations is of fundamental as well as of practical interest. It may, e. g., help in understanding the nature of interference related effects and, for systems with many degrees of freedom (DOF), it may make quantum calculations possible in the first place. The most fundamental approach to reach this goal is based on the application of the semiclassical approximation to the quantum mechanical path integral expression for the time-dependent propagator [1]. A major drawback of the standard time-dependent semiclassical Van Vleck-Gutzwiller formula [2, 3] is the so-called root search problem. One has to find solutions to classical boundary value problems, i. e. classical trajectories connecting a given initial with a given final position in a specified time. This may become numerically cumbersome for longer times, especially if many DOF are involved in the classical dynamics, as is usually the case.

Initial value representations (IVRs) of the semiclassical propagator have therefore been the focus of interest for quite some time [4, 5, 6, 7, 8, 9, 10]. In the IVRs, root searches are avoided by transforming the semiclassical propagator into an integral expression leading to the emergence of classical initial value problems instead of boundary ones. Specifically the Herman-Kluk (HK) IVR expression based on fixed width, i. e. “frozen” Gaussians has been quite successfully applied since its first derivation [6]. Recently, an alternative formulation, based on “thawed” Gaussians, has been brought back into the limelight in Refs. [11] and [12]. The single trajectory version, for a propagated Gaussian in the formulation of Ref. [11] is equivalent to Heller’s Gaussian wave packet dynamics [13], evolving a Gaussian wave packet by using only its center trajectory and allowing the width of the Gaussian to “breathe”. The full integral expression based on thawed Gaussians (i. e. the multitrajectory version, see also Ref. [12]) has already been discussed by Kay [8] and has been labelled thawed Gaussian approximation (TGA). Rather surprisingly, Kay found first numerical evidence that the TGA is numerically far inferior as compared to the HK frozen Gaussian Approximation (HK FGA). As the main result of this article, we propose a “breathing”, individually determined from the global properties of the classical dynamics on the energy shell which is defined for each trajectory by its initial point in phase space, in order to adjust the shortcomings of TGA.

In the following, we will explicitly examine several examples to shed some light on the

reason for the failure of the original TGA. Simultaneously, it will become clearer why FGA is numerically superior. To set the stage, in Sec. II, we briefly review Kay's results [?] of a general semiclassical IVR expression based on coherent states. In Sec. III, the performance of the two special cases, HK FGA and TGA, is contrasted for two different anharmonic test potentials. In Sec. IV, the reason for the TGA failure is underlined by a simple improvement before we introduce the global harmonic approximation which improves TGA to the level of FGA. Conclusions and an outlook are given in Sec. V.

II. SEMICLASSICAL INITIAL VALUE REPRESENTATIONS

A general expression for the quantum propagator, subsuming many of the previously known semiclassical initial value representations, has been derived via the principle of stationary phase equivalence by Kay [8]. He used the fact that the Ansatz as an integral over phase space has to lead to the Van Vleck-Gutzwiller form, if the integration is performed in the stationary phase approximation.

Several early semiclassical approaches, e. g. the ones of Heller [13] and Herman and Kluk [6] are based on Gaussian wave packets of the form

$$\langle x|g_\gamma(p, q)\rangle = \left(\frac{\text{Re}\gamma}{\pi}\right)^{1/4} \exp\left\{-\frac{\gamma}{2}(x-q)^2 + \frac{i}{\hbar}p(x-q)\right\} \quad (1)$$

in coordinate representation. In his seminal work [8], Kay has used these states with arbitrarily time-dependent width parameters $\gamma(t)$ in order to construct a general semiclassical integral expression for the propagator. For our purposes, we need only the special version without a cross term between initial and final Gaussian, given by

$$K(x, t; x', 0) = \int \frac{dp_i dq_i}{2\pi\hbar} \langle x|g_{\gamma_1}(p_t, q_t)\rangle R(p_i, q_i, t) \exp\{iS(p_i, q_i, t)/\hbar\} \langle g_{\gamma_2}(p_i, q_i)|x'\rangle, \quad (2)$$

where the pre-exponential factor,

$$R(p_i, q_i, t) = \left[\frac{1}{2\sqrt{\text{Re}\gamma_1\text{Re}\gamma_2}} \left(\gamma_1 \frac{\partial q_t}{\partial q_i} + \gamma_2 \frac{\partial p_t}{\partial p_i} - i\hbar\gamma_1\gamma_2 \frac{\partial q_t}{\partial p_i} - \frac{1}{i\hbar} \frac{\partial p_t}{\partial q_i}\right)\right]^{1/2} \quad (3)$$

is determined by the stability matrix (or monodromy matrix) elements defined in the matrix equation,

$$\begin{pmatrix} \delta q_t \\ \delta p_t \end{pmatrix} = \begin{pmatrix} \partial q_t/\partial q_i & \partial q_t/\partial p_i \\ \partial p_t/\partial q_i & \partial p_t/\partial p_i \end{pmatrix} \begin{pmatrix} \delta q_i \\ \delta p_i \end{pmatrix} \quad (4)$$

which connect the initial with the final deviations of trajectories (p_t, q_t) in phase space, while the phase is determined by the classical action $S(p_i, q_i, t) = \int_0^t L dt'$ being the time integral over the Lagrange function.

From the general expression, Eq. (2), the HK approximation is recovered by setting $\gamma_1 = \gamma_2 = \gamma$ with a real positive constant γ . The explicit form of the HK FGA prefactor is then

$$R^{\text{HK}}(p_i, q_i, t) = \sqrt{\frac{1}{2} \left(\frac{\partial q_t}{\partial q_i} + \frac{\partial p_t}{\partial p_i} - i\hbar\gamma \frac{\partial q_t}{\partial p_i} - \frac{1}{i\hbar\gamma} \frac{\partial p_t}{\partial q_i} \right)}, \quad (5)$$

while by setting

$$\gamma_1 = -\frac{i \partial p_t / \partial q_i + i\hbar\gamma \partial p_t / \partial p_i}{\hbar \partial q_t / \partial q_i + i\hbar\gamma \partial q_t / \partial p_i} \quad (6)$$

again with real positive γ [14] and $\gamma_2 = \gamma$, we recover the TGA. This semiclassical IVR has recently also been discussed by Baranger et al. [11, 12]. The prefactor turns out to be

$$R^{\text{TGA}}(p_i, q_i, t) = \left(\frac{\gamma}{\text{Re}\gamma_1} \right)^{1/4} \left(\frac{\partial q_t}{\partial q_i} + i\hbar\gamma \frac{\partial q_t}{\partial p_i} \right)^{-1/2}. \quad (7)$$

In the following, we will numerically investigate the TGA expression and compare the results to FGA and full quantum results. Later on, the general expression (2) will then also allow us to search for improvements of the TGA propagator.

III. LONG TIME ACCURACY OF HK FGA VERSUS TGA

For reasons of simplicity, the wave function to be propagated is chosen to be a Gaussian $\Psi(x, 0) = \langle x | g_\gamma(p_0, q_0) \rangle$ localized around (p_0, q_0) in phase space and having the same width parameter as the initial Gaussian in the integral expression of the propagator in Eq. (2) [15]. In the following we will compare the overlap between the time propagated and the unpropagated wavepacket, the so-called autocorrelation function

$$c(t) = \int_{-\infty}^{\infty} dx \Psi^*(x, 0) \Psi(x, t), \quad (8)$$

for the different semiclassical approaches.

Inserting the propagator from Eq. (2), we obtain the semiclassical autocorrelation function

$$c(t) = \int \frac{dq_i dp_i}{2\pi\hbar} \langle g_\gamma(p_0, q_0) | g_{\gamma_1}(p_t, q_t) \rangle R(p_i, q_i, t) \exp \{ iS(p_i, q_i, t) / \hbar \} \langle g_{\gamma_2}(p_i, q_i) | g_\gamma(p_0, q_0) \rangle. \quad (9)$$

The overlap integral between the Gaussians can be performed analytically, whereas the phase space integration in Eq. (9) is done numerically by the Monte Carlo integration procedure described in Ref. [16]. To test the numerical performance of the different methods we chose two different nonlinear potentials which we now introduce.

First, we employ the Hamiltonian taken by Baranger et al. [11] to test their integral kernel,

$$H_B = \frac{p^2}{2\mu} + 2V_0 e^{-\alpha A} \cosh(\alpha x). \quad (10)$$

Throughout the rest of the article, we use only this classical version of the Hamiltonian (without Gaussian smoothing) with (scaled) units, particularly scaled time t_B , indirectly defined by the parameters taken from Ref. [11] as $\mu = 1$, $V_0 = 1$, $A = 5$, $\alpha = 1$, and a Planck constant of $\hbar = 0.05$. The initial conditions of the wave packet are $q_0 = 0$ and $p_0 = 1$ and $\gamma = 100/9$. ‘‘Smoothing’’ of the Hamiltonian by using its coherent state matrix element leads only to minor changes (not shown) in the results to be presented below.

As the second test bed, we choose the well known Morse potential with the Hamiltonian

$$H_M = \frac{p^2}{2\mu} + V_0(1 - e^{-\lambda x})^2 \quad (11)$$

which is a reasonable model for a chemical bond. The parameters taken from Ref. [7] as $\lambda = 0.08$, $V_0 = 30$, which together with $\mu = 1$ define a scaled time t_M . As initial conditions for the wavepacket we define $q_0 = p_0 = 0$ and $\gamma = 12$.

In Fig. 1, we compare different semiclassical IVR results (i. e. using the full integral expression) to the quantum result, calculated by the split operator method, for the two model potentials. For the Baranger potential, we have calculated the autocorrelation function up to scaled times of 110, as displayed in Fig. 1(a). In accord with the decay of the norm in Fig. 1(c), also the autocorrelation function shows a strong decay, not present in the full quantum curve. We state explicitly that the decay of the norm for TGA and also the discrepancy of the norm from unity in the HK FGA case are not in contradiction to the fact that both methods are unitary in the (analytical) stationary phase sense (see e. g., Ref. [17] for the HK FGA case).

Nevertheless, for the Baranger potential, the quality of the numerical TGA results is disappointing. For the very short times (up to 10 in scaled units) investigated in Ref. [11], even the one trajectory (kernel) version of TGA, i. e., Heller’s Gaussian wave packet dynamics, does better than the full integral version (not shown). This method is, however,

not suited for longer times due to the nonlinearity of the potential. In contrast, as can also be observed in Figs. 1(a) and 1 (c), the HK FGA approach gives a reasonable agreement with the full quantum solution.

The same kind of discrepancies of TGA from the quantum split operator calculation as for the Baranger potential can be observed in the case of the Morse potential. The corresponding results are given in Figs. 1 (b) and 1 (d). As has been noted already in [10], for the Morse potential, the HK FGA approximation represents the fine details of the full quantum result very well. The multitrajectory TGA expression, however, already fails again at intermediate times.

IV. IMPROVEMENTS OF THE TGA

With the comparison of the different results at hand, we have the means to find the reason for the poor performance of the TGA expression.

A. Generalized TGA

The reason for the disappointing TGA results becomes clear by taking a closer look at the time-dependent width parameter γ_1 . To this end, we concentrate on the Hamiltonian of Eq.(10) with the Baranger potential. As can be seen in the lower panel of Fig. 2, the real part of the complex width parameter is almost always close to zero for longer times. This leads to a strongly oscillating exponent in the TGA integral expression. Although the Monte Carlo results which we present are converged, the strong oscillation of the integrand leads to the rapid deterioration of the results. The reason for the satisfactory behavior of the HK FGA in the cases we investigated is obviously the fixed real width parameter which by definition does not decay.

This observation opens up a possibility to improve on the standard TGA expression in a simple way. If one could render the width parameter's "destructive influence" on the results less dramatic, this would certainly ameliorate the results. An easy way to achieve this goal is by taking (higher-order) roots of the width parameter γ_1 . This is done in the upper two panels of Fig. 2, where in panel (b)-the square root -and in panel (a) the fourth root of the width parameter in panel (c) is taken. Clearly, the decay of the real part is

less dramatic. The effect that this change has on the autocorrelation function can now be checked by inserting the new width parameter into the general integral expression of Eq. (2) and calculating the resulting prefactor. The emerging propagator is then still semiclassical in the sense of stationary phase equivalence. The numerical results are shown in the upper panels of Fig. 3. Already in the case of the fourth root (see panel Fig. 2 (a)), the generalized TGA result is almost as good as the HK FGA. By making the final Gaussians narrower in width, we have reached an intermediate goal. TGA can now better capture the real quantum dynamics.

There is, however, one further aspect to this improvement. The issue whether the generalized TGA can do as well as HK FGA with fewer trajectories. To study this, we have investigated the convergence of the Monte Carlo integration for FGA, the two different generalized TGAs, and the standard TGA. For the Baranger potential example, all methods require on the order of several times 10^3 trajectories to achieve convergence. The HK FGA needs a slightly higher number of trajectories than standard TGA. Taking roots of higher and higher order makes the width almost constant and, therefore, the TGA propagator approaches the FGA. This also leads to more trajectories which are required for convergence.

Besides taking roots of the width parameter, there is yet another way to improve the TGA, making it a true alternative to the FGA. This approach will be studied in the remainder of this article.

B. Global harmonic approximation

A starting point for an improvement of the TGA, different in spirit from the one presented above, is based on the fact that all *time-dependent* semiclassical approaches become exact for the case of the harmonic oscillator. The TGA is especially favorable for the case of a harmonic potential, whose frequency ω does not coincide with the width parameter of the Gaussians used in the integral expression for the propagator. Already the single trajectory Gaussian wave packet dynamics gives the exact analytical solution (the so-called squeezed state) which breathes (for $\omega \neq \hbar\gamma/\mu$) according to the time-dependent width parameter

$$\gamma_1 = -\frac{i}{\hbar} \frac{-\mu\omega \sin(\omega t) + i\hbar\gamma \cos(\omega t)}{\cos(\omega t) + i\hbar\gamma/(\mu\omega) \sin(\omega t)}. \quad (12)$$

The individual Gaussians of TGA breathe in the same way as the solution does, allowing the convergence of the numerical results to be achieved with fewer trajectories than in the HK FGA case, also explaining the remarks at the end of the previous subsection. Is this observation of any use for realistic non-harmonic potentials?

The answer is yes and we want to demonstrate this for the case of the Morse oscillator with the parameters given in the previous section. For the bound motion in any potential we can define an action variable

$$I = \frac{1}{2\pi} \int_C pdq = \frac{1}{2\pi} \int_C \sqrt{2\mu(E - V)} dq \quad (13)$$

by integrating over a closed contour C in phase space. The Hamiltonian does not depend on the corresponding angle variable and can be expressed as a function of I . Its derivative, with respect to the action variable, then defines a frequency

$$\omega = \frac{\partial H}{\partial I} \quad (14)$$

which in anharmonic potentials depends on energy and, in the simple one DOF case, can be determined analytically. The idea of the improvement of TGA is now to use the oscillation frequency given above as the one of a “fictitious” harmonic oscillator and let every Gaussian breathe with the corresponding γ_1 . While all stability matrix elements for the calculation of the semiclassical propagator are taken to be the harmonic ones, the trajectories themselves are propagated using the full nonlinear force field. For every trajectory, the approximation is a *global* harmonic approximation, with respect to the stability information. Note that the present approach is different from the the so-called nonlinear Gaussian wave packet dynamics, introduced by Tomsovic and Heller [18] which uses a *local* expansion of the potential up to second order (as Heller’s original Gaussian wave packet dynamics) and is not an IVR formulation but a root search method in spirit.

We are now using the global harmonic approximation for the width parameter and also the prefactor in Eq. (9) to calculate the autocorrelation function in the Morse oscillator case. The results are shown in Fig. 4. A dramatic improvement toward the HK FGA result can be observed. The reason is that now γ_1 behaves as in the harmonic case, i. e. it does not decay to zero for later times, thus leading to reasonable results. We found that the same kind of improvement toward HK is also present for wave packets with different initial conditions (not shown).

V. CONCLUSIONS

Based on numerical studies for two different anharmonic potentials (Baranger and Morse), we have identified the decay of the width parameters of the Gaussians in time as the reason for the failure of the TGA to provide a good semiclassical propagator. Following this notion, we have introduced the global harmonic approximation which mimics for each trajectory its stability properties in time according to those of a harmonic oscillator. Its frequency is defined through an action-angle analysis of the dynamics on the energy shell set by the initial conditions of each trajectory. The TGA, amended by the global harmonic approximation for the stability of trajectories, is comparable in accuracy to the HK FGA propagator.

More detailed studies, e. g. of the convergence properties of the different methods, on the choice of an optimal width parameter γ for FGA, and on the applicability of the improved TGA also to unbound problems are worthwhile topics for future investigations.

Acknowledgements

We would like to thank Rick Heller and Eli Pollak for useful discussions.

-
- [1] R. P. Feynman and A. R. Hibbs, *Quantum Mechanics and Path Integrals* (McGraw-Hill, New York, NY, 1965).
- [2] J. H. Van Vleck, Proc. Acad. Nat. Sci. USA **14**, 178 (1928).
- [3] M. C. Gutzwiller, J. Math. Phys. **8** 1979 (1967).
- [4] W. H. Miller, J. Chem. Phys. **53** (1970) 1949; J. Phys. Chem. A **105** (2001) 2942.
- [5] E. J. Heller, J. Chem. Phys. **75**, 2923 (1981).
- [6] M. F. Herman, E. Kluk, Chem. Phys. **91**, 27 (1984).
- [7] E. J. Heller, J. Chem. Phys. **94**, 2723 (1991).
- [8] K. G. Kay, J. Chem. Phys. **100**, 4377 (1994).
- [9] K. G. Kay, J. Chem. Phys. **100**, 4432 (1994); *ibid.* **101**, 2250 (1994).
- [10] F. Grossmann, Comments At. Mol. Phys. **34**, 141 (1999).
- [11] M. Baranger et al., J. Phys. A:Math. Gen. **34**, 7227 (2001).
- [12] M. Baranger et al., J. Phys. A:Math. Gen. **35**, 9493 (2002).
- [13] E. J. Heller, J. Chem. Phys. **62** (1975) 1544.
- [14] γ can be also taken complex if the real part is positive; a slight generalization of the final result is then necessary [8]
- [15] Especially for TGA this is *not* the optimum choice for the numerics but there is no straightforward way to optimize the width parameter and therefore, we stick to this simple choice.
- [16] E. Kluk, M. Herman and H. L. Davis, J. Chem. Phys. **84**, 326 (1986).
- [17] M. Herman, J. Chem. Phys. **85**, 2069 (1986).
- [18] S. Tomsovic and E. J. Heller, Phys. Rev. E **47**, 282 (1993).

FIG. 1: Comparison of different semiclassical versus quantum autocorrelation functions and the semiclassical results for the norm for the Baranger potential (a) and (c) and the Morse potential (b) and (d) with the potential parameters given in the text. Full line: quantum result, dashed line: HK FGA, dotted line: TGA

FIG. 2: The real part of the time dependent width parameter in the TGA expression: (c) standard γ_1 , (b) $\tilde{\gamma}_1 = \sqrt{\gamma_1}$, (a) $\bar{\gamma}_1 = \gamma_1^{1/4}$.

FIG. 3: The standard and generalized TGA results in the case of the Baranger potential according to the prefactors in Fig. 2. Full line: quantum result, dotted line: TGA

FIG. 4: The global harmonic TGA result compared to the HK FGA results for the Morse oscillator. Dashed line: HK FGA, dotted line TGA, and full line: global harmonic TGA

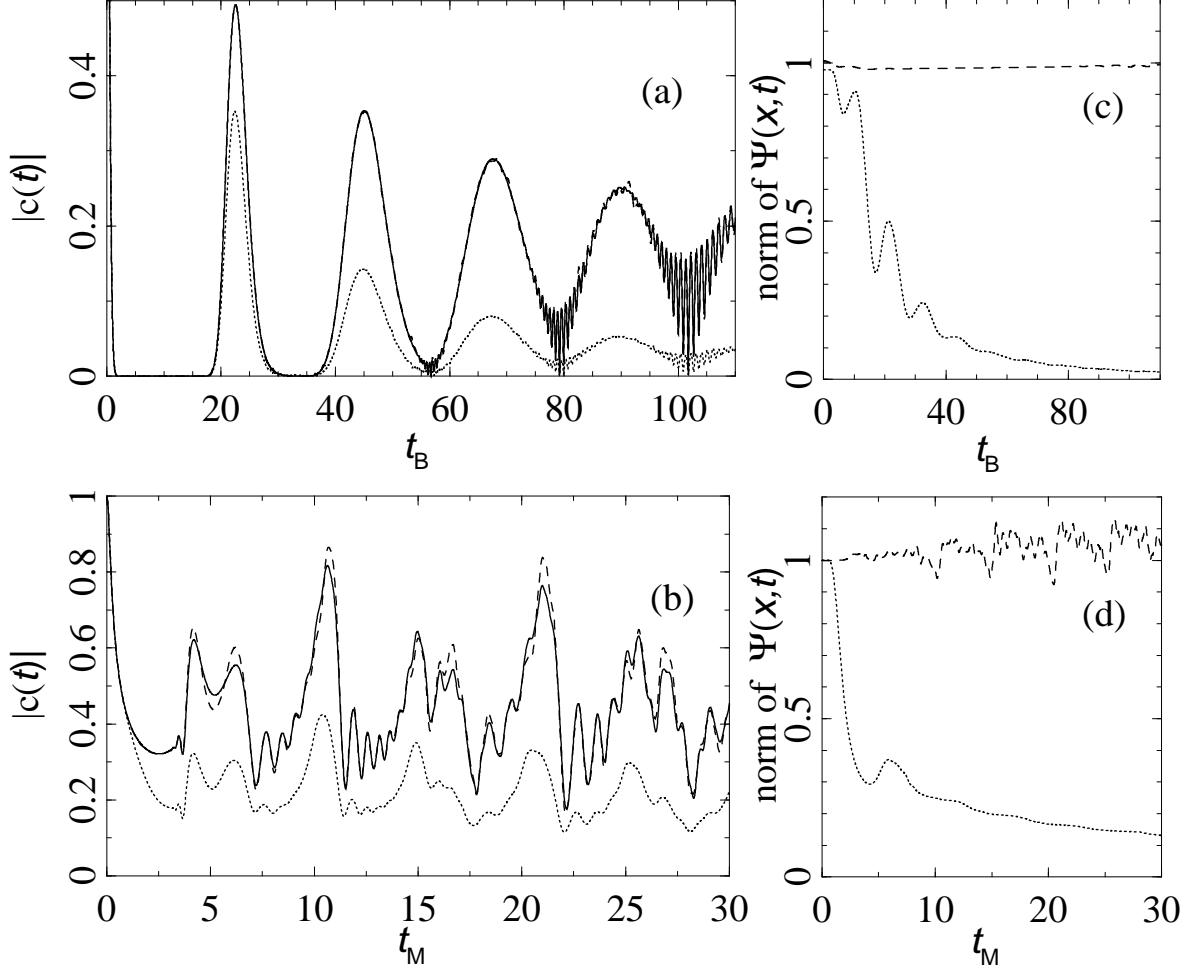


FIG. 1: Comparison of different semiclassical versus quantum autocorrelation functions and the semiclassical results for the norm for the Baranger potential (a) and (c) and the Morse potential (b) and (d) with the potential parameters given in the text. Full line: quantum result, dashed line: HK FGA, dotted line: TGA

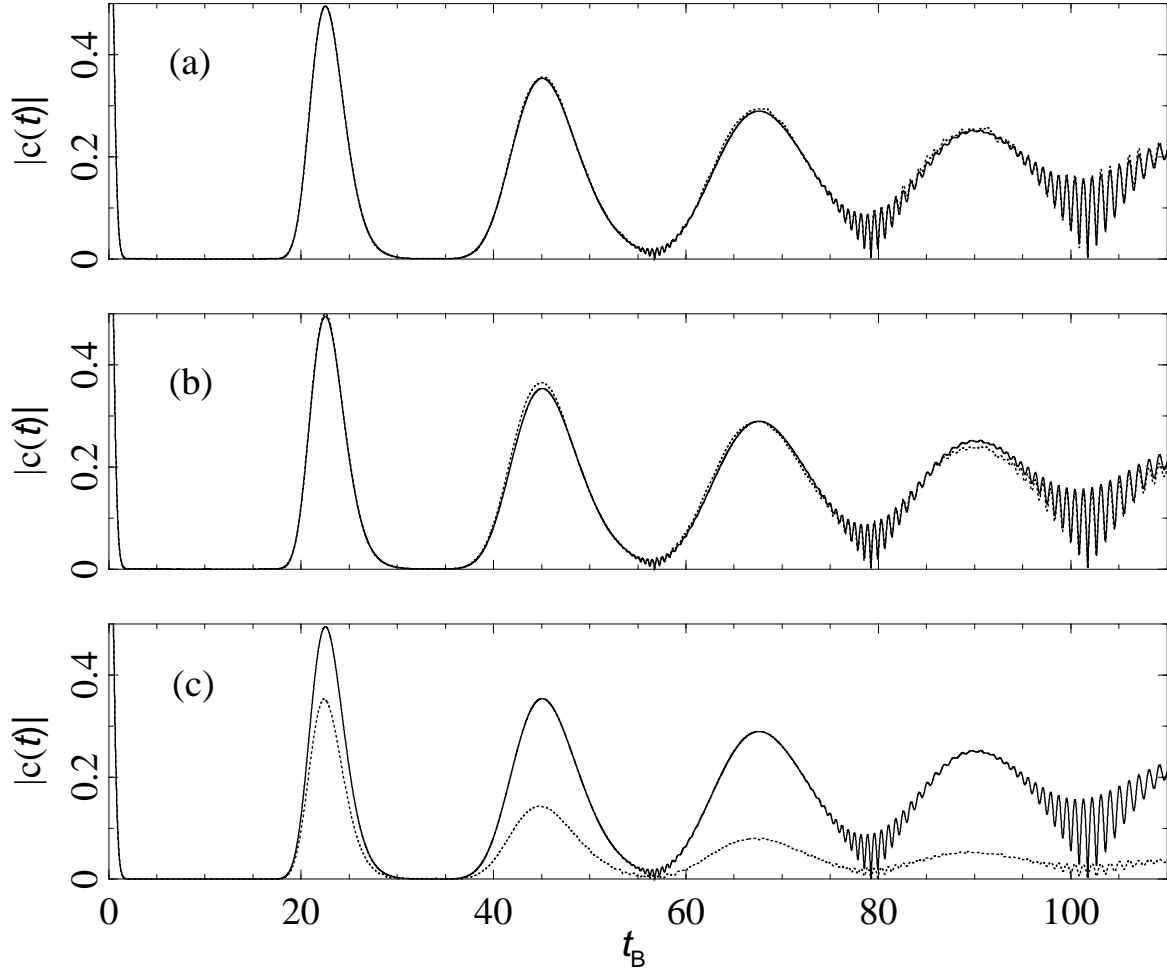


FIG. 3: The standard and generalized TGA results in the case of the Baranger potential according to the prefactors in Fig. 2. Full line: quantum result, dotted line: TGA

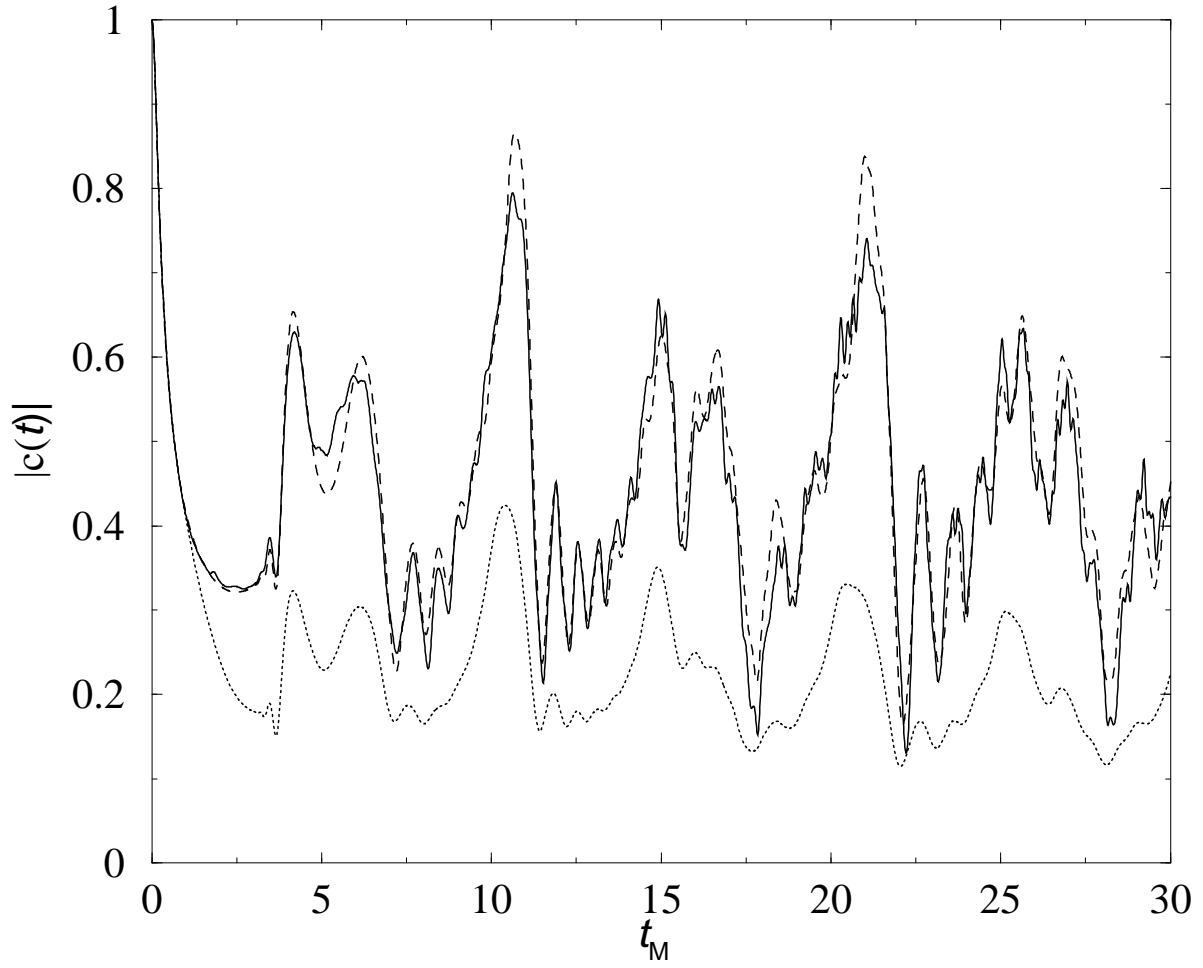


FIG. 4: The global harmonic TGA result compared to the HK FGA results for the Morse oscillator. Dashed line: HK FGA, dotted line TGA, and full line: global harmonic TGA